Measurement of Heteronuclear Coupling Constants in Organometallic Complexes Using High-Resolution 2D NMR

Nick Bampos, Leslie D. Field,* and Barbara A. Messerle

Department of Organic Chemistry, University of Sydney, Sydney 2006, NSW, Australia

Received November 17, 1992

^1H–^{31}P coupling constants across the central metal atom ($^2J_{P-M-H}$) were measured in a series of octahedral hydridometal phosphine complexes [$MRH(PP_3)$, $PP_3 = P(CH_2CH_2CH_2P(CH_3)_2)_3$; M = Ru, Fe; R = H, Cl, 1-pentenyl, cyclopentenyl, 2-methyl-1-butenyl, 3,3-dimethyl-1-butenyl] using a selective two-dimensional NMR experiment. The use of band-selective pulses focused on a narrow frequency range in the ^1H NMR spectrum (encompassing the metal-bound hydride resonances) provided spectra with high resolution as well as removed the need for suppression of intense signals arising from protic organic solvents. The magnitude of $^2J_{P-M-H}$ was found to depend on the relative disposition of the coupled nuclei and about the central metal atom, as well as the nature of the metal. For $FeRH(PP_3)$ complexes, the magnitude of $^2J_{P-M-H(cis)} > {}^2J_{P-M-H(trans)}$, while for analogous Ru complexes, $^2J_{P-M-H(trans)} > {}^2J_{P-M-H(cis)}$. Irrespective of whether the metal center is Fe or Ru, the sign of $^2J_{P-M-H(trans)}$ is opposite that of $^2J_{P-M-H(cis)}$ and $^2J_{P-M-P(cis)}$, but the same as $^2J_{P-M-P(trans)}$.

Introduction

The measurement of coupling constants is an important and essential part of the characterization of organic and organometallic compounds by NMR spectroscopy. In organometallic compounds, the magnitude of homo- and heteronuclear coupling constants can provide information about the stereochemistry of metal complexes as well as the oxidation state and coordination geometry of the central metal atom.[1,2] The relative magnitude of ^{31}P–^{31}P coupling constants in hexacoordinate iron(II) phosphine complexes is characteristic of the configuration of groups around the iron center with $^2J_{P-M-P(trans)} > {}^2J_{P-M-P(cis)}$ and $^2J_{P-M-P(trans)}$ of sign opposite that of $^2J_{P-M-P(cis)}$.[2] Early work suggested that similar trends were apparent in the heteronuclear ^{31}P–^1H coupling constants ($^2J_{P-M-H}$) in transition metal complexes containing both phosphine and hydride ligands.[1]

Both homonuclear and heteronuclear coupling constants are sensitive to the electronic structure of bonded atoms and molecular geometry in terms of dihedral angles.[3–5] Heteronuclear coupling constants, *e.g.* $^3J_{C-\alpha H}$ and $^3J_{N-C-H}$ are now widely used to provide additional constraints for the calculation of three-dimensional structures.[6]

A number of NMR techniques are now available to facilitate the measurement of coupling constants,[7,8] and these include homonuclear 2D experiments such as ECOSY,[8,9] selective excitation methods,[10] and heteronuclear 2D and 3D experiments.[6,11,12] All rely ultimately on the careful measurement of the line separations between either in-phase or antiphase components of multiplets for the measurement of the J coupling constants. With antiphase signals, the peak separation can be affected by signal cancellation when the line width is significant relative to the peak separation.[13,14] ECOSY,[8,9] PCOSY,[15] selective variants of DQF-COSY[10,16] and heteronuclear sequences[6,17] overcome the problem by creating cross-peak patterns where the peak separation defining the coupling constant is defined by peaks with the same phase. Special methods for measuring heteronuclear coupling constants (X–H) have been developed[12,18] particularly for applications using isotopically labeled proteins.[19]

In this paper we describe the measurement of heteronuclear (^{31}P–^1H) coupling constants, and their relative signs, in a series of organometallic complexes $MRH(PP_3)$, [$PP_3 = P(CH_2CH_2CH_2P(CH_3)_2)_3$, M = Ru, Fe] using a band-selective, proton-detected two-dimensional X–H correlation experiment. The 2D experiment has the advantage that narrow sweep widths in the proton dimension can be achieved, and this permits the analysis of the high-resolution structure of cross-peak multiplets.

(1) (a) Moore, D. S.; Robinson, S. D. *Chem. Soc. Rev.* **1983**, *12*, 415. (b) Kaesz, H. D.; Saillant, R. B. *Chem. Rev.* **1972**, *72*, 231.
(2) Field, L. D.; Baker, M. V. *Inorg. Chem.* **1987**, *26*, 2011.
(3) Güntert, P.; Braun, W.; Billeter, M.; Wüthrich, K. *J. Am. Chem. Soc.* **1989**, *111*, 3997.
(4) Karplus, M. *J. Am. Chem. Soc.* **1963**, *85*, 2870.
(5) Bystrov, V. F. *Prog. NMR Spectrosc.* **1976**, *10*, 41.
(6) Schmieder, P.; Thanabal, V.; McIntosh, L. P.; Dahlquist, F. W.; Wagner, G. *J. Am. Chem. Soc.* **1991**, *113*, 6323.
(7) (a) Bax, A.; Freeman, R. *J. Magn. Reson.* **1981**, *44*, 542. (b) Oschkinat, H.; Pastore, A.; Pfaendler, P.; Bodenhausen, G. *J. Magn. Reson.* **1986**, *69*, 559. (c) Mueller, L. *J. Magn. Reson.* **1987**, *71*, 191.
(8) Griesinger, C.; Sorensen, O. W.; Ernst, R. R. *J. Am. Chem. Soc.* **1985**, *107*, 6394.
(9) Griesinger, C.; Sorensen, O. W.; Ernst, R. R. *J. Magn. Reson.* **1987**, *75*, 474.
(10) (a) Brueschweiler, R.; Madsen, J. C.; Griesinger, C.; Sorensen, O. W.; Ernst, R. R. *J. Magn. Reson.* **1987**, *73*, 380. (b) Emsley, L.; Bodenhasuen, G. *J. Am. Chem. Soc.* **1991**, *113*, 3309. (c) Bodenhausen, G.; Freeman, R.; Morris, G. A. *J. Magn. Reson.* **1976**, *23*, 171.
(11) Titman, J. J.; Neuhaus, D.; Keeler, J. *J. Magn. Reson.* **1989**, *85*, 111.
(12) (a) Kessler, H.; Mronga, S.; Gemmecker, G. *Magn. Reson. Chem.* **1991**, *29*, 527. (b) Kessler, H.; Anders, U.; Gemmecker, G. *J. Magn. Reson.* **1988**, *78*, 382.
(13) Neuhaus, D.; Wagner, G.; Vasak, M.; Kaegi, J. H. R.; Wüthrich, K. *Eur. J. Biochem.* **1985**, *151*, 257.
(14) Widmer, H.; Wüthrich, K. *J. Magn. Reson.* **1986**, *70*, 270.
(15) Bax, A.; Freeman, R. *J. Magn. Reson.* **1981**, *44*, 542.
(16) Piantini, U.; Sorensen, O. W.; Ernst, R. R. *J. Am. Chem. Soc.* **1982**, *104*, 6800.
(17) (a) Titman, J. J.; Keeler, J. *J. Magn. Reson.* **1990**, *89*, 640. (b) Gemmecker, G.; Fesik, S. W. *J. Magn. Reson.* **1991**, *95*, 208.
(18) (a) Montelione, G. T.; Wagner, G. *J. Am. Chem. Soc.* **1989**, *111*, 5474. (b) Sklenar, V.; Bax, A. *J. Am. Chem. Soc.* **1987**, *109*, 7525. (c) Neri, D.; Otting, G.; Wüthrich, K. *J. Am. Chem. Soc.* **1990**, *112*, 3663.
(19) (a) Montelione, G. T.; Winkler, M. E.; Rauenbuehler, P.; Wagner, G. *J. Magn. Reson.* **1989**, *82*, 198. (b) Sorensen, O. W. *J. Magn. Reson.* **1990**, *90*, 433. (c) Chary, K. V. R.; Otting, G.; Wüthrich, K. *J. Magn. Reson.* **1991**, *93*, 218.

0276-7333/93/2312-2529$04.00/0

Results and Discussion

Hydrocarbon activation has been achieved with a number of transition metal complexes.[20] Where the product metal complexes are thermally unstable or short lived, it is necessary to obtain as much structural information as possible on the products *in situ* in solution before isolation or derivatization.

The tripodal ligand $P(CH_2CH_2CH_2P(CH_3)_2)_3$[21a] forms one-to-one octahedral complexes with Fe^{2+} and Ru^{2+}.[21b,c] The complex $H_2FeP(CH_2CH_2CH_2P(CH_3)_2)_3$ (**1a**) is fluxional in solution at room temperature, and its dynamic behavior has been studied in detail.[22] In a preliminary account of C–H activation with the Fe and Ru dihydride complexes[23] $H_2FeP(CH_2CH_2CH_2P(CH_3)_2)_3$ (**1a**) and $H_2RuP(CH_2CH_2CH_2P(CH_3)_2)_3$ (**2a**) under photochemical conditions, it was reported that **2a** activated arenes to give arylruthenium hydrides but that **1a** failed to intermolecularly activate hydrocarbons. When irradiated at room temperature in solution, **1a** undergoes an intramolecular cyclometalation.[23a]

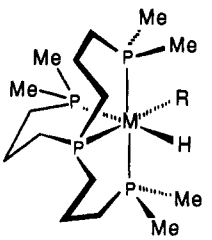

(1) M = Fe
(2) M = Ru

a	R = H
b	R = Cl
c	R = *(E)*-1-pentenyl
d	R = *(Z)*-1-pentenyl
e	R = *(E)*-2-methyl-1-pentenyl
f	R = *(Z)*-2-methyl-1-pentenyl
g	R = cyclopentenyl
h	R = *(E)*-3,3-dimethyl-1-butenyl

When irradiated at low temperature, **1a** activates C—H bonds in alkenes, forming alkenyl metal hydride species which are stable only at low temperatures (below 240 K). The complexes **1c**, **1g**, and **1h** were obtained by irradiation of **1a** in the appropriate (neat) alkene solvent, and activation was complete with 2–4 h of irradiation at 220 K.[25] In contrast to alkene activation which has been reported for other iron tetraphosphines,[24] only products derived from activation of the alkene sp^2 C—H bonds were observed; *i.e.* no π-bound products which would arise from direct activation of the C=C π-system were detected. For the iron complexes **1c** and **1h** the products obtained had exclusively the *(E)*-stereochemistry about C=C. The *(E/Z)*-stereochemistry of the products about the alkenyl C=C was established from the magnitude of the proton—proton $^3J_{H-C=C-H}$ coupling between the olefin protons. Complexes with the *(E)*-stereochemistry had $^3J_{H-C=C-H}$ coupling constants in the range 16–17 Hz and in the corresponding *(Z)*-isomers this coupling was significantly less (*ca.* 12.5 Hz).

Alkene activation with the ruthenium complex **2a** afforded mixtures of *(E)*- and *(Z)*-isomers, with the *(E)*-isomer being the major product for all alkenes examined. Formation of the Ru complexes required irradiation for 20–24 h. The complexes **2c–2g** were more thermally stable than the corresponding iron complexes, and they could be formed and manipulated at room temperature. In all of the alkene complexes examined, the vinylic protons of the metal-bound alkenyl fragments exhibited broadening due to $^{31}P-^1H$ coupling (*ca.* 2–4 Hz).

The complexes **1c**, **1g**, **1h**, and **2c–g** are previously unknown compounds, and the configuration of the complexes at the metal center was established unambiguously by $^1H-^1H$ NOE experiments.[26] ^{31}P spectra were assigned on symmetry grounds, and the methyl resonances in the ^1H NMR spectra were assigned using standard 2D $^{31}P-^1H$ heteronuclear correlation experiments. In $^1H-^1H$ NOE experiments, the alkenyl substituent shows a strong interaction with the methyl substituents on the unique terminal phosphorus atom and the hydride ligand shows strong interactions with the methyl substituents of the equivalent axial phosphorus ligands and not with the methyl substituents on the unique terminal phosphorus atom. In all cases examined, the product complexes form with the alkenyl substituents *trans* to the apical phosphorus atom of the tripodal ligand.

NMR Spectroscopy Using Frequency-Selective Pulses

Heteronuclear coupling constants, $^2J_{P-H}$ or $^3J_{P-H}$, for phosphinometal hydrides have conventionally been obtained by spectral simulation of the observed hydride and phosphorus spectra, combined with selective decoupling of the ^{31}P resonances. In complex systems, where resonances are too close or where the magnitude of P–H coupling constants is large, selective decoupling of the heteronuclear resonances is not possible. Selective decoupling is also inconclusive where there are mixtures of compounds or where there is a high degree of overlap of resonances in either the ^1H or ^{31}P spectra.

Frequency-selective (band-selective) pulses are now routinely available for NMR spectroscopy,[10,27–29] and

(20) See for example: (a) Hoyano, J. K.; McMaster, A. D.; Graham, W. A. G. *J. Am. Chem. Soc.* **1983**, *105*, 7190. (b) Jones, W. D.; Feher, F. J. *Organometallics* **1983**, *2*, 562. (c) Wenzel, T. T.; Bergman, R. G. *J. Am. Chem. Soc.* **1986**, *108*, 4856. (d) Graham, W. A. G. *J. Organomet. Chem.* **1986**, *300*, 81. (e) Baker, M. V.; Field, L. D. *J. Am. Chem. Soc.* **1987**, *109*, 2825. (f) Field, L. D.; George, A. V.; Messerle, B. A. *J. Chem. Soc., Chem. Commun.* **1991**, *19*, 1339. (g) *Selective Hydrocarbon Activation; Principles and Progress*; Davies, J. A., Watson, P. L., Liebman, J. F., Greenberg, A., Eds.; VCH Publishers, Inc.: New York, 1990 (see also references therein). (h) *Activation and Functionalisation of Alkanes*; Hill, C. L., Ed.; Wiley Interscience: New York, 1989 (see also references therein).

(21) (a) Antberg, M.; Dahlenburg, L.; Prengel, C. *Inorg. Chem.* **1984**, *23*, 4170. (b) Antberg, M.; Dahlenburg, L. *Inorg. Chim. Acta* **1985**, *104*, 51. (c) Antberg, M.; Dahlenburg, L. *Inorg. Chim. Acta* **1986**, *111*, 73.

(22) Field, L. D.; Bampos, N.; Messerle, B. A. *Magn. Reson. Chem.* **1991**, *29*, 36.

(23) (a) Antberg, M.; Dahlenberg, L. *Angew. Chem., Int. Ed. Engl.* **1986**, *25*, 260. (b) Antberg, M.; Dahlenberg, L.; Frosin, K.-M.; Höck, N. *Chem. Ber.* **1988**, *121*, 859.

(24) (a) Baker, M. V.; Field, L. D. *J. Am. Chem. Soc.* **1986**, *108*, 7433. (b) Baker, M. V.; Field, L. D. *J. Am. Chem. Soc.* **1986**, *108*, 7436. (c) Baker, M. V.; Ph.D. Thesis, University of Sydney, 1987.

(25) Samples were irradiated in Pyrex NMR tubes positioned approximately 10 cm from a 125-W mercury vapor lamp. The tubes were suspended in a vacuum-jacketed Pyrex cylinder and cooled by a stream of nitrogen gas.

(26) (a) Young, G. B.; James, T. L. *J. Am. Chem. Soc.* **1984**, *106*, 7986. (b) *The Nuclear Overhauser Effect in Structural and Conformational Analysis*; Neuhaus, D., Williamson, W., Eds.; VCH Publishers, Inc.: New York, 1989. (c) Field, L. D.; Bampos, N.; Messerle, B. A. Manuscript in preparation.

(27) Friedrich, J.; Davies, S.; Freeman, R. *J. Magn. Reson.* **1987**, *75*, 390.

(28) Geen, H.; Wimperis, S.; Freeman, R. *J. Magn. Reson.* **1989**, *85*, 620.

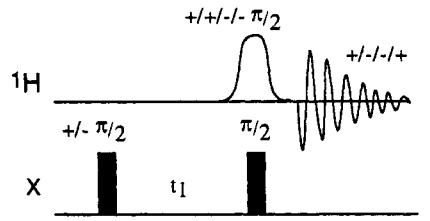

Figure 1. Pulse sequence used for acquisition of selective X–H correlation spectra. The phase cycling indicated was rotated in a CYCLOPS cycle,[31] and phase-sensitive acquisition was achieved using TPPI[32] by incrementing the phase of the first pulse to the heteronucleus (X) by $\pi/2$ for each slice of the 2D data set acquired.

Gaussian pulses and their derivatives[12a,27] are the most widely used. However, for experiments where it is essential to maintain the shape of the peaks selected with minimal phase or intensity distortion, Gaussian-shaped pulses are poor and the self-refocusing shaped pulses such as E-BURP[28,29] are superior.

In this work, a modification of a basic two-dimensional X–H correlation pulse sequence[30] (Figure 1) was employed with proton detection and the final pulse to ^{1}H replaced by a selective E-BURP pulse.

The two hard pulses applied to the heteronuclei effectively label proton magnetization with the heteronuclear chemical shifts. Polarization transfer to protons coupled to heteronuclei (inverse INEPT) employed an E-BURP pulse to excite only a narrow band of ^{1}H frequencies (200–400 Hz) centered on the region of the metal-bound hydride. The two-dimensional spectrum obtained has a narrow spectral window in F_2 (^{1}H) and the complete heteronuclear spectral range in F_1 (^{31}P). During the evolution delay (τ_1) ^{31}P magnetization evolves as a complex function of ^{31}P shifts as well as ^{31}P–^{31}P couplings and ^{1}H–^{31}P couplings. Providing τ_1 is sampled for sufficiently long that the value of $1/\tau_{1(max)}$ is comparable to (or greater than) the smallest expected heteronuclear coupling constant, the whole range of heteronuclear coupling constants is efficiently sampled in this experiment. This pulse sequence with no preset delays provides an advantage over those experiments which require evolution over specific periods since fixed delays can only be optimized for a narrow range of coupling constants. The use of selective pulses in the proton domain afforded two-dimensional spectra with high digital resolution across the multiplets of the metal-bound protons. In addition, the selective pulses permitted NMR measurements to be made in neat protonated organic solvents where the intense proton resonances of the solvent were not excited.

A range of metal complexes (**1a–c**, **1g**, **1h**, **2a–g**) was examined using the selective ^{31}P–^{1}H correlation experiment (Figure 1), where the selective pulse was centered on the resonances of the metal-bound proton(s). The resulting two-dimensional spectrum of compound **1a** is shown in Figure 2. The cross-peaks contain both positive and negative components, and the antiphase components identify the active ^{31}P–^{1}H coupling constant and hence the ^{31}P resonance which gives rise to it.

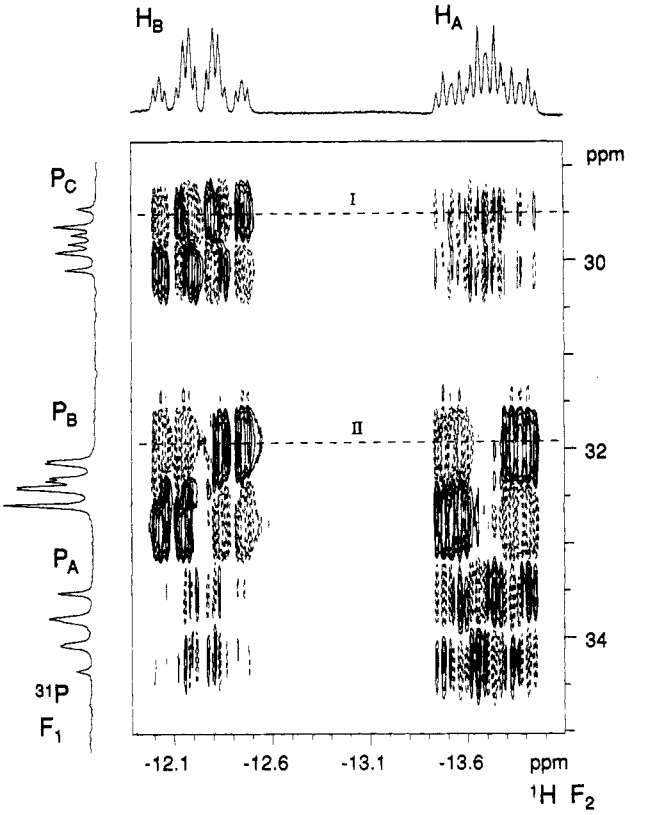

Figure 2. ^{1}H-detected two-dimensional X–H correlation experiment of $Fe(PP_3)H_2$ (**1a**) obtained using the pulse sequence in Figure 1 with the selective E-BURP pulse centered at the midpoint of the metal-bound hydride resonances (400 MHz, toluene-d_8 solvent, 220 K). Dashed lines are negative contours. Cross-sections at I and II are shown in Figure 3b,c respectively. The one-dimensional ^{31}P spectrum on the F_1 axis was acquired with ^{1}H decoupling.

In **1a**, each hydride is coupled to the equivalent axial phosphorus nuclei, to the central apical phosphorus atom, and to the terminal phosphorus in the equatorial plane of the complex. The ^{1}H NMR of **1a** shows each of the metal-bound hydrides as a 24-line multiplet (dddt) as the result of ^{31}P–^{31}P coupling and ^{1}H–^{1}H coupling between the hydrides. The two-dimensional spectrum shows one cross-peak between each hydride resonance and each nucleus in the ^{31}P spectrum. At the frequency of each resonance (P_x) in the ^{31}P spectrum, the structure of the cross-peak is complex but in any row of the cross-peak, only those multiplet splittings arising from the active coupling (to P_x) are antiphase and all other splittings are in-phase. The pattern of in-phase and antiphase components in the cross-peaks of the two-dimensional map uniquely assigns the ^{31}P–^{1}H coupling which arises from each ^{31}P nucleus.

Two representative rows (cross-sections in F_2) from the phase-sensitive two-dimensional spectrum in Figure 2 are shown in Figure 3. Figure 3b shows the section through the resonances of H_A and H_B at the frequency of P_C. For H_B, the P–H doublet splitting of 47.3 Hz is antiphase while the multiplet components for all other couplings are in-phase, and this identifies the 47.3-Hz splitting as due to $^2J_{P(C)-Fe-H(B)}$. At H_A, the smallest P–H doublet splitting (14.0 Hz) is antiphase identifying this as $^2J_{P(C)-Fe-H(A)}$. At the frequency of the equivalent axial phosphorus nuclei (P_B), the outer wings of the P–H triplet are clearly antiphase for both H_A and H_B. For triplet splittings, the central line of the multiplet are nulled in this type of inverse INEPT sequence.

(29) Geen, H.; Freeman, R. *J. Magn. Reson.* **1991**, *93*, 93.
(30) Maudsley, A. A.; Ernst, R. R. *Chem. Phys. Lett.* **1977**, *50*, 368.
(31) (a) Hoult, D. I.; Richards, R. E. *Proc. R. Soc.* London **1975**, *A344*, 311. (b) Bodenhausen, G.; Kogler, H.; Ernst, R. R. *J. Magn. Reson.* **1984**, *58*, 370.
(32) (a) Drobny, G.; Pines, A.; Sinton, S.; Weitekamp, D.; Wemmer, D. *Faraday Div. Chem. Soc. Symp.* **1979**, *13*, 49. (b) Bodenhausen, G.; Vold, R. L.; Vold, R. R. *J. Magn. Reson.* **1980**, *37*, 93.

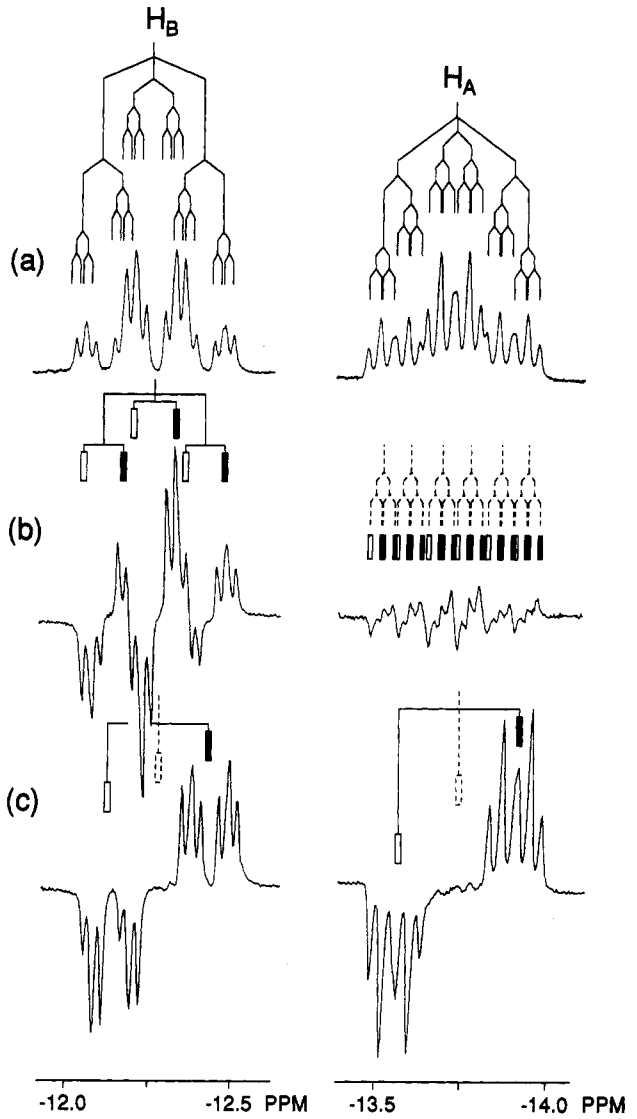

Figure 3. Selected F_2 cross-sections through the two-dimensional X–H correlation spectrum (Figure 2): (a) basic ^1H spectrum (b) cross-section through the multiplet at the ^{31}P frequency of P_C (indicated by I in Figure 2), and (c) cross-section through the multiplet at the ^{31}P frequency of P_B (indicated by II in Figure 2).

The heteronuclear couplings can be measured directly from the two-dimensional spectrum (Figure 2), or appropriate cross-sections (Figure 3). However, once the spectral assignments have been made, more precise values of the coupling constants can be obtained by computer simulation of a high-resolution ^1H spectrum.

Magnitude of P–M–H Coupling Constants. The measured magnitudes of the ^{31}P–^1H coupling constants for a series of $MRH(PP_3)$ complexes are given in Table I.

For the range of iron(II) complexes examined, the values of $^2J_{P-M-H}$ for the coupling between the metal-bound hydride and ligand phosphorus nuclei were internally consistent across the series. With the axial direction defined as that occupied by the mutually *trans* phosphine substituents, the magnitude of the *cis* coupling between the equatorial hydride and the axial phosphines ($^2J_{P(B)-M-H(cis)} \sim 60$–$70$ Hz) is significantly larger than the *cis* coupling between groups in the equatorial plane ($^2J_{P(A)-M-H(cis)} \sim 30$–$36$ Hz), or the *trans* coupling ($^2J_{P(C)-M-H(trans)} \sim 14$–$32$ Hz). For compound **1a** the relative magnitudes of the coupling constants remain internally consistent for both hydrides with the coupling from either hydride to phosphorus in the *trans* position being significantly smaller than other couplings and the *cis* coupling to the axial phosphorus atoms being the largest. Similarly, within the series of ruthenium complexes **2a–2f**, the coupling constants are internally consistent. However, in contrast to the analogous Fe complexes, the magnitudes of the *cis* coupling between the metal-bound equatorial hydride and the ^{31}P in the equatorial plane ($^2J_{P(A)-M-H(cis)} = 17$–23 Hz) and the *cis* coupling between the equatorial hydride and the axial phosphines ($^2J_{P(B)-M-H(cis)} = 12$–31 Hz) are significantly smaller than the *trans* coupling to the remaining ^{31}P in the equatorial plane ($^2J_{P(C)-M-H(trans)} = 68$–$96$ Hz).

The tetradentate phosphine ligand $P(CH_2CH_2CH_2P(CH_3)_2)_3$ constrains Fe(II) and Ru(II) complexes in a relatively inflexible geometry. The structures of those Fe(II) and Ru(II) complexes containing this ligand, which have been studied by crystallography[33] and by NMR spectroscopy,[26c] are remarkably similar. For both metal centers the X-ray crystal structure data suggest that the complexes adopt distorted octahedral geometries with metal–phosphorus bond lengths between 2.20 and 2.33 Å for Fe and 2.28 and 2.34 Å for Ru.[33] Differences in the relative sizes of the heteronuclear coupling constants between first and second row transition metals have been attributed to differences in the ligand geometry, *i.e.* significant distortion of the shape of the coordination sphere.[1b,34] The observed inversion in the relative magnitudes of *cis* and *trans* heteronuclear ^{31}P–^1H coupling from Fe to Ru complexes is unlikely to be due to the minor differences in geometry and must arise from other factors such as the difference in the Fe and Ru outer electron orbital configurations.

Relative Signs of P–M–H Coupling Constants. The relative signs of homonuclear and heteronuclear coupling constants in organometallic chemistry have been established for only a few complexes.[34] In homonuclear spin systems, the most commonly used techniques for establishing the relative signs of coupling constants are the COSY-45[35] and E-COSY[8,9] experiments. Selective DQF-COSY[16] experiments have also been employed.

The selective two-dimensional heteronuclear correlation experiment depicted in Figure 1 is analogous to a homonuclear COSY experiment, and replacement of the final 90° pulse to the X nucleus (^{31}P) by a 45° pulse makes the experiment sensitive to the relative signs of the X–H (and X–X) coupling constants. The cross-peaks in a spectrum acquired with a pulse sequence containing a 45° pulse show a reduced number of signals compared to the typical cross-peak achieved using a 90° pulse (Figure 2). The position or pattern of peak absences depends on the relative signs of the coupling constants contributing to the cross-peak.[36] The passive couplings to each of the nuclei giving rise to a cross-peak include heteronuclear couplings (J_{P-H} in F2) as well as homonuclear couplings (J_{P-P} in F1).[2,36] Figure 4 shows an expansion of the fine detail of the experimental P_B–H_A multiplets of 2D spectra of compound

(33) (a) Antberg, M.; Dahlenburg, L. *Acta Crystallogr.* **1986**, C42, 997. (b) Antberg, M.; Dahlenburg, L.; Frosin, K.-M.; Hoeck, N. *Chem. Ber.* **1988**, *121*, 859.

(34) See for example: (a) Pregosin, P. S.; Kunz, R. W. *NMR: Basic Princ. Prog.* **1979**, *15*, 28–34, 86 and references therein. (b) Verkade, J. G. *Coord. Chem. Rev.* **1972/73**, *9*, 1. (c) Goodfellow, R. J.; Taylor, B. F. *J. Chem. Soc., Dalton Trans.* **1974**, 1676. (d) Pankowski, M.; Chodkiewicz, W.; Simonnin, M-P. *Inorg. Chem.* **1985**, *24*, 533.

(35) Bax, A.; Freeman, R. *J. Magn. Reson.* **1981**, *44*, 542.

Table I. Relative Magnitudes of Heteronuclear $^{31}P-^{1}H$ Coupling Constants (Hz) for the Hydride Resonances of $FeRHP(CH_2CH_2CH_2P(CH_3)_2)_3$ and $RuRHP(CH_2CH_2CH_2P(CH_3)_2)_3$ Complexes

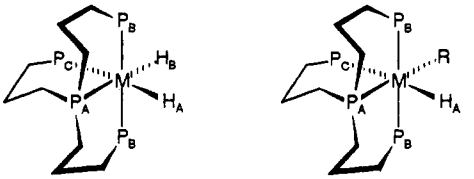

M	complex	R	$^{2}J_{P(A)-M-H(A)}$	$^{2}J_{P(B)-M-H(A)}$	$^{2}J_{P(C)-M-H(A)}$
Fe[a]	**1a**	H_B	32.9	70.2	14.0
Fe	**1b**	Cl	37.8	70.5	30.8
Fe	**1c**	(*E*)-CH=CHCH$_2$CH$_2$CH$_3$	36.9	72.4	29.8
Fe	**1g**	cyclopentenyl	45.8	67.4	31.3
Fe	**1h**	(*Z*)-CH=CHC(CH$_3$)$_3$	36.6	71.2	29.6
Ru[b]	**2a**	H_B	22.5	12.1	68.1
Ru	**2b**	Cl	22.4	28.5	95.6
Ru	**2c**	(*E*)-CH=CHCH$_2$CH$_2$CH$_3$	17.9	30.8	80.9
Ru	**2d**	(*Z*)-CH=CHCH$_2$CH$_2$CH$_3$	17.0	29.7	85.5
Ru	**2e**	(*E*)-CH=C(CH$_3$)CH$_2$CH$_2$CH$_3$	17.4	29.4	84.9
Ru	**2f**	(*Z*)-CH=C(CH$_3$)CH$_2$CH$_2$CH$_3$	17.7	28.5	85.8
Ru	**2g**	cyclopentenyl	19.3	29.0	84.9

[a] $Fe(PP_3)H_2$, $^{2}J_{P(A)-Fe-H(B)} = 12.2$, $^{2}J_{P(B)-Fe-H(B)} = 59.6$, $^{2}J_{P(C)-Fe-H(B)} = 47.3$, $^{2}J_{H(A)-Fe-H(B)} = 13.3$ Hz. [b] $Ru(PP_3)H_2$, $^{2}J_{P(A)-Ru-H(B)} = 56.9$, $^{2}J_{P(B)-Ru-H(B)} = 16.2$, $^{2}J_{P(C)-Ru-H(B)} = 21.8$, $^{2}J_{H(A)-Ru-H(B)} < 2$ Hz.

2c acquired using both 90 and 45° pulses in the pulse sequence in Figure 1.

Figure 4a shows a schematic representation of the (P_B–H_A) cross-peak obtained using the pulse sequence in Figure 1 with a 90° pulse as the final pulse to ^{31}P. The multiplet components in F_2 (^{1}H) are antiphase with respect to the active P–H (triplet) coupling for this multiplet ($^{2}J_{P(B)-M-H(A)}$) and in-phase with respect to the other P–H (doublet) couplings. The multiplet components in F_1 (^{31}P) are in-phase with respect to the P–P (doublet) couplings and antiphase with respect to the active P–H (doublet) coupling ($^{2}J_{P(B)-M-H(A)}$). In the corresponding experimental spectrum (Figure 4c), there is considerable overlap between the multiplet components in F_1 due to poor digital resolution and broadening due to additional proton coupling. When the complete 2D spectrum is simulated[37] with an enlarged line width in F_1 to accommodate resonance overlap (Figured 4e), the simulated and experimental spectra are virtually superimposable. For the simulations, the magnitudes of the various couplings were taken directly from Table I with $^{2}J_{P(A)-M-H(A)}$, $^{2}J_{P(B)-M-H(A)}$, $^{2}J_{P(A)-M-P(B)}$, $^{2}J_{P(A)-M-P(C)}$, $^{2}J_{P(B)-M-P(C)}$ negative and $^{2}J_{P(C)-M-H(A)}$, $^{2}J_{P(B)-M-P(B)}$ positive. The intense peaks form four "sub-spectral squares"[36] which are offset from each other by the passive splittings; the relative positions of the sub-spectral squares is a function of the relative signs of the passive coupling constants contributing to the multiplet. The corresponding section of the experimental spectrum is given in Figure 4d, and the complete simulated[37] spectrum (Figure 4f) is again virtually superimposable. The match of the simulated and experimental spectra depends critically on the relative signs of the passive coupling constants, and only where $^{2}J_{P(A)-M-H(A)}$, $^{2}J_{P(B)-M-H(A)}$, $^{2}J_{P(A)-M-P(B)}$, $^{2}J_{P(A)-M-P(C)}$, $^{2}J_{P(B)-M-P(C)}$ have signs opposite those of $^{2}J_{P(C)-M-H(A)}$ and $^{2}J_{P(B)-M-P(B)}$ can a match be obtained.

The relative signs of the heteronuclear $^{2}J_{P-M-H}$ couplings were determined for compounds **1a**, **1c**, **2c**, and **2d**. In six-coordinate complexes, two-bond, phosphorus–phosphorus coupling constants, $^{2}J_{P-M-P}$, are characteristic of the stereochemical relationship between the phosphine ligands as well as the nature of the metal–ligand bonding in the complex. Typically, the magnitude of $^{2}J_{P-M-P(trans)}$, is greater than that of $^{2}J_{P-M-P(cis)}$, with $^{2}J_{P-M-P(trans)}$ having a positive sign and $^{2}J_{P-M-P(cis)}$ a negative sign.[1,2,34] Relative to the sign of $^{2}J_{P-M-P(cis)}$, in complexes **1a**, **1c**, **2c**, and **2d**, $^{2}J_{P-M-H(trans)}$ has an opposite sign and $^{2}J_{P-M-H(cis)}$ an identical sign. This trend in the relative signs of coupling constants was apparent for all the complexes examined, irrespective of the metal center (Fe/Ru) or whether the interaction was between axial/axial ligands or axial/equatorial ligands and can be summarized as follows: $^{2}J_{P-M-P(trans)} > 0$, $^{2}J_{P-M-P(cis)} < 0$, $^{2}J_{P-M-H(cis)} < 0$, $^{2}J_{P-M-H(trans)} > 0$.

Conclusions

A heteronuclear pulse sequence incorporating a band-selective E-BURP pulse enabled high-resolution two-dimensional $^{1}H-^{31}P$ NMR spectra of iron and ruthenium hydrides to be obtained. Heteronuclear $^{31}P-^{1}H$ coupling constants were assigned and measured from the detailed structure of the complex cross-peak multiplets.

This is the first systematic study which has examined heteronuclear coupling in a range of similar octahedral iron and ruthenium tetraphosphines in sufficient detail that the relative magnitudes and signs of heteronuclear $^{31}P-^{1}H$ coupling constants could be measured. In both iron and ruthenium complexes, the heteronuclear coupling constants are diagnostic of the relative disposition of the coupled nuclei in the octahedral coordination sphere of the metal. The largest $^{2}J_{P-M-H}$ coupling is between the metal hydride and the phosphorus substituent *trans* to it in Ru complexes but the largest $^{2}J_{P-M-H}$ coupling is between the metal hydride and the *cis* axial phosphorus substituents in the series of Fe complexes. For both Ru and Fe complexes, the relative sign of the coupling $^{2}J_{P-M-H(trans)}$

(36) (a) Ernst, R. R.; Bodenhausen, G.; Wokaun, A. *Principles of Nuclear Magnetic Resonance in One and Two Dimensions*; Oxford University Press: Oxford, U.K., 1987; pp 414–22. (b) Bax, A. *Two Dimensional NMR in Liquids*; Delft University Press, D. Reidel Publishing Co.: Delft, Holland, 1982; pp 78–84.

(37) Struder, W. *J. Magn. Reson.* **1988**, *77*, 424. 2D simulations were performed using the computer subroutine SMART running within the program UXNMRP (Bruker Spectrospin) running on a SUN Sparcstation. Spectra of **2c** were simulated using the P–H coupling constants in Table I and the P–P couplings measured directly from the $^{31}P\{^{1}H\}$ spectrum.

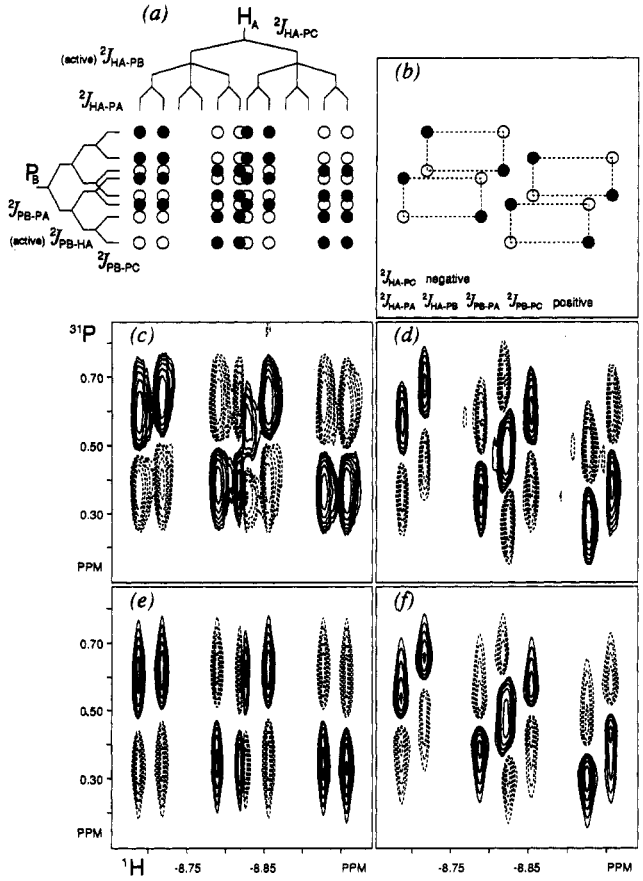

Figure 4. Selected cross-peak P_B–H_A of the two-dimensional X-H correlation spectrum of **2c**. (a) Schematic representation of the P_B–H_A cross-peak with a 45° pulse as the final pulse to ^{31}P in the pulse sequence in Figure 1. Filled circles are positive peaks; open circles are negative peaks. (b) Schematic representation of the P_B–H_A cross-peak with a 45° pulse as the final pulse to ^{31}P in the pulse sequence in Figure 1. (c) Experimental cross-peak P_B–H_A from the two-dimensional X–H correlation with 90° pulses (Figure 1). (d) As for (c) but with a 45° pulse as the final pulse to ^{31}P. (e) Computer simulation[37] of the experimental multiplet in Figure 4c. (f) Computer simulation[37] of the experimental multiplet in Figure 4d with $^2J_{P(A)-M-H(A)}$, $^2J_{P(B)-M-H(A)}$, $^2J_{P(A)-M-P(B)}$, $^2J_{P(A)-M-P(C)}$, $^2J_{P(B)-M-P(C)}$ negative and $^2J_{P(C)-M-H(A)}$, $^2J_{P(B)-M-P(B)}$ positive.

is opposite that of $^2J_{P-M-H(cis)}$ and $^2J_{P-M-P(cis)}$ but the same as that of $^2J_{P-M-P(trans)}$.

Experimental Section

1-Pentene, 2-methyl-1-pentene, cyclopentene, and 3,3-dimethyl-1-butene (Aldrich) were distilled and degassed by three freeze–pump–thaw cycles before use.

NMR Spectroscopy. Spectra of the iron complexes (**1a**, **1b**, **1g**, and **1h**) were acquired at 222 K in toluene-d_8 while those of complex **1b** and the ruthenium complexes (**2a**–**2g**) were acquired at room temperature in toluene-d_8. Selective E-BURP pulses[28,29] were applied using the soft pulse hardware of a Bruker AMX400 or AMX600 spectrometer. ^{31}P NMR spectra were referenced to external, neat trimethyl phosphite, taken as 140.85 ppm at the temperature quoted; ^1H NMR spectra were referenced to residual solvent resonances. Shaped pulses were defined by 256 points, centered on the resonance(s) of the metal-bound hydrides in the ^1H spectrum. Selective pulses were typically between 5 and 15 ms in duration, giving excitation widths of approximately 200–1200 Hz. In 2D acquisitions, typically, 2048 data points were acquired over a sweep width of 1500 Hz in the ^1H spectrum, with 256 increments and 64 scans per increment. A relaxation delay of 2.5 s was left between acquisitions. Spectra were zero-filled to 512 points in F_1 and 4096 points in F_2. Sine-bell weightings were applied to the data in both dimensions (shifted by $\pi/2$ in F_2 and $\pi/4$ in F_1) prior to Fourier transformation.

Metal Complexes. **$FeCl_2P(CH_2CH_2CH_2P(CH_3)_2)_3$** was prepared following literature methods.[21b,38]

$FeHClP(CH_2CH_2CH_2P(CH_3)_2)_3$ (1b) was prepared by the partial reduction of $FeCl_2P(CH_2CH_2CH_2P(CH_3)_2)_3$ with a THF solution of $LiAlH_4$.[38] $FeHClP(CH_2CH_2CH_2P(CH_3)_2)_3$ (**1b**): $^{31}P\{^1H\}$ NMR (toluene-d_8, 303 K) δ 60.6 (dt, 1P, P_A, $^2J_{P(A)-M-P(B)}$ = 65.5, $^2J_{P(A)-M-P(C)}$ = 48.1 Hz), 18.7 (dd, 2P, P_B, $^2J_{P(B)-M-P(C)}$ = 25.8 Hz), 9.6 (dt, 1P, P_C); $^1H\{^{31}P\}$ NMR (toluene-d_8, 303 K) δ 1.61, 1.52, 0.84 (3 × m, 3 × 2H, 3 × $-CH_2-$), 1.86, 1.76, 1.72, 1.26, 1.04, 0.84 (6 × m, 6 × 1H, 6 × $-CHH-$), 1.62 (s, 6H, 2 × $-CH_3$), 2.13, 1.56 (2 × s, 2 × 3H, 2 × $-CH_3$), −10.4 (s, 1H, Fe–H).

$FeH_2P(CH_2CH_2CH_2P(CH_3)_2)_3$ (1a) was obtained by further reduction of the hydrochloride **1b** following the procedure reported by Antburg *et al.*[23a,40] The compound was purified by sublimation (80 °C, <10^{-5} mmHg) to give **1a** as a pale yellow solid. $FeH_2P(CH_2CH_2CH_2P(CH_3)_2)_3$ (**1a**): $^{31}P\{^1H\}$ NMR (toluene-d_8, 240 K) δ 33.6 (dt, 1P, P_A, $^2J_{P(A)-M-P(B)}$ = 48.2, $^2J_{P(A)-M-P(C)}$ = 36.1 Hz), 32.0 (dd, 2P, P_B, $^2J_{P(B)-M-P(C)}$ = 28.9 Hz), 29.5 (dt, 1P, P_C); $^1H\{^{31}P\}$ NMR (toluene-d_8, 240 K) δ 1.87, 1.45, 1.34 (3 × m, 3 × 2H, 3 × $-CH_2-$), 1.98, 1.90, 1.70, 1.50, 1.48, 1.33 (6 × m, 6 × 1H, 6 × $CHH-$), 1.39 (s, 6H, 2 × $-CH_3$), 1.68, 1.40 (2 × s, 2 × 3H, 2 × $-CH_3$), −12.32 (d, 1H, $^2J_{H-Fe-H}$ = 13.3 Hz, Fe–H_B), −13.77 (d, 1H, Fe–H_A).

$RuH_2P(CH_2CH_2CH_2P(CH_3)_2)_3$ (2a) and $RuHClP(CH_2CH_2CH_2P(CH_3)_2)_3$ (2b) were prepared following a previously published procedure.[21c] $RuHClP(CH_2CH_2CH_2P(CH_3)_2)_3$ (**2b**): $^{31}P\{^1H\}$ NMR (toluene-d_8, 303 K) δ 27.3 (dt, 1P, P_A, $^2J_{P(A)-M-P(B)}$ = 39.7, $^2J_{P(A)-M-P(C)}$ = 28.2 Hz), −5.9 (dd, 2P, P_B, $^2J_{P(B)-M-P(C)}$ = 22.4 Hz), −15.3 (dt, 1P, P_C); $^1H\{^{31}P\}$ NMR (toluene-d_8, 303 K) δ 1.68, 1.48, 1.13 (3 × m, 3 × 2H, 3 × $-CH_2-$), 1.90, 1.78, 1.67, 1.39, 1.31, 1.12 (6 × m, 6 × 1H, 6 × $-CHH-$), 1.52 (s, 6H, 2 × $-CH_3$), 2.01, 1.45 (2 × s, 2 × 3H, 2 × $-CH_3$), −7.7 (s, 1H, Fe–H). $RuH_2P(CH_2CH_2CH_2P(CH_3)_2)_3$ (**2a**): $^{31}P\{^1H\}$ NMR (toluene-d_8, 303 K) δ 5.1 (dt, 1P, P_A, $^2J_{P(A)-M-P(B)}$ = 32.0, $^2J_{P(A)-M-P(C)}$ = 23.8 Hz), 5.5 (dd, 2P, P_B, $^2J_{P(B)-M-P(C)}$ = 28.7 Hz), −0.9 (dt, 1P, P_C); $^1H\{^{31}P\}$ NMR (toluene-d_8, 303 K) δ 1.89, 1.53, 1.40 (3 × m, 3 × 2H, 3 × $-CH_2-$), 2.05, 1.83, 1.73, 1.51, 1.50, 1.43 (6 × m, 6 × 1H, 6 × $-CHH-$), 1.47 (s, 6H, 2 × $-CH_3$), 1.75, 1.40 (2 × s, 2 × 3H, 2 × $-CH_3$), −9.45 (d, $^2J_{H-Ru-H}$ < 2 Hz, 1H, Ru–H_A), −8.20 (d, 1H, Ru–H_B).

$FeH((E)\text{-}CH{=}CHCH_2CH_2CH_3)P(CH_2CH_2CH_2P(CH_3)_2)_3$ (1c). A solution of $FeH_2P(CH_2CH_2CH_2P(CH_3)_2)_3$ (**1a**) (*ca.* 10 mg, 0.021 mmol) in neat 1-pentene (0.5 mL) was irradiated[25] at 220 K for 2 h. After this time, ^{31}P NMR indicated that **1a** had been consumed completely and the resulting solution contained the 1-pentenyl hydride **1c** as the sole product. The product was unstable and decomposed on warming to room temperature. The solvent was removed under high vacuum at low temperature (<220 K, ethanol/dry ice bath), and the residue was redissolved in toluene-d_8 condensed onto the sample, maintaining the temperature below 220 K. $FeH((E)\text{-}CH{=}CHCH_2CH_2CH_3)P(CH_2CH_2CH_2P(CH_3)_2)_3$ (**1c**): $^{31}P\{^1H\}$ NMR (toluene-d_8, 222K) δ 28.6 (dt, 1P, P_A, $^2J_{P(A)-M-P(B)}$ = 48.2, $^2J_{P(A)-M-P(C)}$ = 36.1 Hz), 26.5 (dd, 2P, P_B, $^2J_{P(B)-M-P(C)}$ = 28.4 Hz), 24.2 (dt, 1P, P_C); $^1H\{^{31}P\}$ NMR (toluene-d_8, 222 K) δ 7.19 (d, 1H, Fe—CH=C, $^3J_{H-C=C-H}$ = 16.2), 5.58 (dt, 1H, Fe—C=CH–), 2.60 (dt, 2H, C=CH—CH_2–), 1.80 (m, 2H, C=CH—CH_2—CH_2–), 1.26 (t, 3H, –CH_2—CH_3), 1.73, 1.44, 1.15 (3 × m, 3 × 2H, 3 × $-CH_2-$), 1.90, 1.78, 1.62, 1.33, 1.32, 1.31 (6 × m, 6 × 1H, 6 × $-CHH-$), 1.28 (s, 6H, 2 × $-CH_3$), 2.13, 1.23 (2 × s, 2 × 3H, 2 × $-CH_3$), −13.50 (s, 1H, Fe—H).

$FeH(C_5H_7)P(CH_2CH_2CH_2P(CH_3)_2)_3$ (1g). A solution of $FeH_2P(CH_2CH_2CH_2P(CH_3)_2)_3$ (**1a**) (*ca.* 10 mg, 0.021 mmol) in neat cyclopentene (0.5 mL) was irradiated[25] at 220 K for 3 h. After this time, ^{31}P NMR indicated that **1a** had been completely

(38) Bampos, N.; Field, L. D.; Hambley, T. W. *Polyhedron* **1992**, *11*, 1213.
(39) Antberg, M.; Frosin, K.-M.; Dahlenberg, L. *Z. Naturforsch.* **1985**, *40B*, 1485.
(40) Antberg, M.; Frosin, K.-M.; Dahlenberg, L. *J. Organomet. Chem.* **1988**, *338*, 319.

consumed and the resulting solution contained the cyclopentenyl hydride **1g** as the sole product. The product was unstable and decomposed on warming to room temperature. The solvent was removed under high vacuum at low temperature (<220 K, ethanol/dry ice bath), and the residue was redissolved in toluene-d_8 condensed onto the sample, maintaining the temperature below 220 K. $FeH(C_5H_7)P(CH_2CH_2CH_2P(CH_3)_2)_3$, (**1g**): $^{31}P\{^1H\}$ NMR (toluene-d_8, 222 K) δ 26.8 (bm, 2P, P_B), 25.5 (bm, 1P, P_A), 13.0 (bm, 1P, P_C); $^1H\{^{31}P\}$ NMR (toluene-d_8, 222 K) δ 5.59 (t, 1H, Fe—C=C*H*), 2.82 (dt, 2H, C=CH—CH_2–), 2.18 (m, 2H, C=CH—CH$_2$—CH_2–), 2.50 (t, 1H, Fe—C—CH_2–), 1.77, 1.44, 1.14 (3 × m, 3 × 2H, 3 × –CH$_2$–), 1.97, 1.80, 1.64, 1.40, 1.38, 1.27 (6 × m, 6 × 1H, 6 × –C*H*H–), 1.40 (s, 6H, 2 × –CH$_3$), 1.54, 1.17 (2 × s, 2 × 3H, 2 × –CH$_3$), –13.75 (s, 1H, Fe—H).

FeH((*E*)-CH=CHC(CH$_3$)$_3$)P(CH$_2$CH$_2$CH$_2$P(CH$_3$)$_2$)$_3$ (1h). A solution of $FeH_2P(CH_2CH_2CH_2P(CH_3)_2)_3$ (**1a**) (*ca.* 10 mg, 0.021 mmol) in neat 3,3-dimethyl-1-butene (0.5 mL) was irradiated[25] at 220 K for 4 h. After this time, ^{31}P NMR indicated that **1a** had been completely consumed and the resulting solution contained the 3,3-dimethyl-1-butenyl hydride product **1h** as the sole product. The product was unstable and decomposed on warming to room temperature. The solvent was removed under high vacuum at low temperature (<220 K, ethanol/dry ice bath), and the residue was redissolved in toluene-d_8 condensed onto the sample, maintaining the temperature below 220 K. FeH((*E*)-CH=CHC(CH$_3$)$_3$)P(CH$_2$CH$_2$CH$_2$P(CH$_3$)$_2$)$_3$ (**1h**): $^{31}P\{^1H\}$ NMR (toluene-d_8, 222 K) δ 27.6 (dt, 1P, P_A, $^2J_{P(A)-M-P(B)}$ = 49.4, $^2J_{P(A)-M-P(C)}$ = 36.0 Hz), 25.0 (dd, 2P, P_B, $^2J_{P(B)-M-P(C)}$ = 27.5, Hz), 23.2 (dt, 1P, P_C); $^1H\{^{31}P\}$ NMR (toluene-d_8, 222 K) δ 7.15 (d, 1H, Fe—C*H*=C, $^3J_{H-C=C-H}$ = 17.0 Hz), 5.60 (dt, 1H, Fe—C=C*H*–), 1.50 (s, 9H, –(CH_3)$_3$), 1.79, 1.48, 1.20 (3 × m, 3 × 2H, 3 × –CH$_2$–), 1.97, 1.84, 1.70, 1.40, 1.36, 1.24 (6 × m, 6 × 1H, 6 × –C*H*H–), 1.34 (s, 6H, 2 × –CH$_3$), 1.64, 1.26 (2 × s, 2 × 3H, 2 × –CH$_3$), –13.50 (s, 1H, Fe—H).

RuH((*E*)-CH=CHCH$_2$CH$_2$CH$_3$)P(CH$_2$CH$_2$CH$_2$P(CH$_3$)$_2$)$_3$ (2c) and RuH((*Z*)-CH=CHCH$_2$CH$_2$CH$_3$)P(CH$_2$CH$_2$CH$_2$P-(CH$_3$)$_2$)$_3$ (2d). A solution of $RuH_2P(CH_2CH_2CH_2P(CH_3)_2)_3$ (**2a**) (*ca.* 10 mg, 0.019 mmol) in neat 1-pentene was irradiated[25] at room temperature for 20 h. After this time, ^{31}P NMR indicated 90% conversion of **2a** and the resulting solution contained a mixture of the 1-pentenyl hydrides **2c** and **2d** in the approximate ratio 4:3. The product mixture was stable in solution at room temperature. The solvent was removed under high vacuum and the product dissolved in toluene-d_8. The complexes **2c** and **2d** were examined as a mixture by ^{31}P and ^1H NMR spectroscopy. RuH((*E*)-CH=CHCH$_2$CH$_2$CH$_3$)P(CH$_2$CH$_2$CH$_2$P(CH$_3$)$_2$)$_3$ (**2c**): $^{31}P\{^1H\}$ NMR (toluene-d_8, 303 K) δ 1.67 (dt, 1P, P_A, $^2J_{P(A)-M-P(B)}$ = 33.8, $^2J_{P(A)-M-P(C)}$ = 24.0 Hz), 0.46 (dd, 2P, P_B, $^2J_{P(B)-M-P(C)}$ = 24.0 Hz), –6.22 (dt, 1P, P_C); $^1H\{^{31}P\}$ NMR (toluene-d_8, 303 K) δ 7.44 (d, 1H, Ru—C*H*=C, $^3J_{H-C=C-H}$ = 16.6 Hz), 5.71 (dt, 1H, Ru—C=C*H*–), 2.44 (dt, 2H, C=CH—CH_2–), 1.75 (m, 2H, C=CH—CH$_2$—CH_2–), 1.34 (t, 3H, –CH$_2$—CH_3), 2.35, 2.06, 1.94 (3 × m, 3 × 2H, 3 × –CH$_2$–), 2.39, 2.32, 2.25, 2.14, 2.03, 1.77 (6 × m, 6 × 1H, 6 × –C*H*H–), 1.76 (s, 6H, 2 × –CH$_3$), 1.81, 1.67 (2 × s, 2 × 3H, 2 × –CH$_3$), –8.82 (s, 1H, Ru—H). RuH((*Z*)-CH=CHCH$_2$CH$_2$CH$_3$)P(CH$_2$CH$_2$CH$_2$P(CH$_3$)$_2$)$_3$ (**2d**): $^{31}P\{^1H\}$ NMR (toluene-d_8, 303 K) δ 1.66 (dd, 2P, P_B, $^2J_{P(A)-M-P(B)}$ = 32.0, $^2J_{P(B)-M-P(C)}$ = 24.0 Hz), 1.02 (dt, 1P, P_A, $^2J_{P(A)-M-P(C)}$ = 24.0 Hz), –7.07 (dt, 1 P, P_C); $^1H\{^{31}P\}$ NMR (toluene-d_8, 303 K) δ 7.64 (d, 1H, Ru—C*H*=C, $^3J_{H-C=C-H}$ = 12.5 Hz), 6.64 (dt, 1H, Ru—C=C*H*–), 2.71 (dt, 2H, C=CH—CH_2–), 1.82 (m, 2H, C=CH—CH$_2$—CH_2–), 1.41 (t, 3H, –CH$_2$—CH_3), 2.35, 2.06, 1.94 (3 × m, 3 × 2H, 3 × –CH$_2$–), 2.39, 2.32, 2.25, 2.14, 2.03, 1.77 (6 × m, 6 × 1H, 6 × –C*H*H–), 1.76 (s, 6H, 2 × –CH$_3$), 1.86, 1.73 (2 × s, 2 × 3H, 2 × –CH$_3$), –8.47 (ddt, 1 H, Ru—H).

RuH((*E*)-CH=C(CH$_3$)CH$_2$CH$_2$CH$_3$)P(CH$_2$CH$_2$CH$_2$P-(CH$_3$)$_2$)$_3$ (2e) and RuH((*Z*)-CH=C(CH$_3$)CH$_2$CH$_2$CH$_3$)P(CH$_2$-CH$_2$CH$_2$P(CH$_3$)$_2$)$_3$ (2f). A solution of $RuH_2P(CH_2CH_2CH_2P-(CH_3)_2)_3$ (**2a**) (*ca.* 10 mg, 0.019 mmol) in neat 2-methyl-1-pentene was irradiated[25] at room temperature for 20 h. After this time, ^{31}P NMR indicated 90% conversion of **2a** and the resulting solution contained a mixture of the 2-methyl-1-pentenyl hydrides **2e** and **2f** in the approximate ratio 4:3. The product mixture was stable in solution at room temperature. The solvent was removed under high vacuum and the product dissolved in toluene-d_8. The complexes **2e** and **2f** were examined as a mixture by ^{31}P and ^1H NMR spectroscopy. RuH((*E*)-CH=C(CH$_3$)CH$_2$CH$_2$CH$_3$)P(CH$_2$-CH$_2$CH$_2$P(CH$_3$)$_2$)$_3$ (**2e**): $^{31}P\{^1H\}$ NMR (toluene-d_8, 303 K) δ 3.00 (dd, 2P, P_B, $^2J_{P(A)-M-P(B)}$ = 34.7, $^2J_{P(B)-M-P(C)}$ = 24.5 Hz), 1.92 (dt, 1P, P_A, $^2J_{P(A)-M-P(C)}$ = 24.5 Hz), –6.48 (dt, 1P, P_C); $^1H\{^{31}P\}$ NMR (toluene-d_8, 303 K) δ 7.19 (s, 1H, Ru—C*H*=C), 2.46 (s, 3H, Ru—C=C(CH_3)–), 2.73 (dt, 2H, C=C(CH$_3$)—CH_2–), 2.34 (m, 2H, –CH$_2$—CH_2—CH$_3$), 1.35 (t, 3H, –CH$_2$—CH_3), 1.90, 1.60, 1.38 (3 × m, 3 × 2H, 3 × –CH$_2$–), 2.17, 1.87, 1.81, 1.55, 1.40, 1.38 (6 × m, 6 × 1H, 6 × –C*H*H–), 1.41 (s, 6H, 2 × –CH$_3$), 1.63, 1.31, (2 × s, 2 × 3H, 2 × –CH$_3$), –8.61 (s, 1H, Ru—H). RuH((*Z*)-CH=C(CH$_3$)CH$_2$CH$_2$CH$_3$)P(CH$_2$CH$_2$CH$_2$P(CH$_3$)$_2$)$_3$ (**2f**): $^{31}P\{^1H\}$ NMR (toluene-d_8, 303 K) δ 1.90 (dd, 2P, P_B, $^2J_{P(A)-M-P(B)}$ = 35.0, $^2J_{P(B)-M-P(C)}$ = 23.7 Hz), 1.16 (dt, 1P, P_A, $^2J_{P(A)-M-P(C)}$ = 23.7, Hz), –8.61 (dt, 1P, P_C); $^1H\{^{31}P\}$ NMR (toluene-d_8, 303 K) δ 7.22 (s, 1H, Ru—C*H*=C), 2.50 (s, 3H, Ru—C=C(CH_3)–), 2.91 (dt, 2H, C=C(CH$_3$)—CH_2–), 2.02 (m, 2H, –CH$_2$—CH_2—CH$_3$), 1.46 (t, 3H, –CH$_2$—CH_3), 1.90, 1.60, 1.38 (3 × m, 3 × 2H, 3 × –CH$_2$–), 2.17, 1.87, 1.81, 1.55, 1.40, 1.38 (6 × m, 6 × 1H, 6 × –C*H*H–), 1.41 (s, 6H, 2 × –CH$_3$), 1.63, 1.31 (2 × s, 2 × 3H, 2 × –CH$_3$), –8.57 (s, 1H, Ru—H).

RuH(C$_5$H$_7$)P(CH$_2$CH$_2$CH$_2$P(CH$_3$)$_2$)$_3$ (2g). A solution of $RuH_2P(CH_2CH_2CH_2P(CH_3)_2)_3$ (**2a**) (*ca.* 10 mg, 0.019 mmol) in neat cyclopentene was irradiated[25] at room temperature for 20 h. After this time, ^{31}P NMR indicated >90% conversion of **2a** and the resulting solution contained the cyclopentenyl hydride **2g** as the sole product. The product was stable in solution at room temperature. The solvent was removed under high vacuum and the product dissolved in toluene-d_8. RuH(C$_5$H$_7$)P(CH$_2$CH$_2$-CH$_2$P(CH$_3$)$_2$)$_3$ (**2g**): $^{31}P\{^1H\}$ NMR (toluene-d_8, 303 K) δ 26.8 (bm, 2P, P_B), 25.5 (bm, 1P, P_A), 13.0 (bm, 1P, P_C); $^1H\{^{31}P\}$ NMR (toluene-d_8, 303 K) δ 5.66 (d, 1H, Ru—C=C*H*), 2.74 (dt, 2H, C=CH—CH_2–), 2.12 (m, 2H, C=CH—CH$_2$—CH_2–), 2.64 (t, 1H, Fe—C—CH_2–), 1.79, 1.48, 1.22 (3 × m, 3 × 2H, 3 × –CH$_2$–), 1.98, 1.78, 1.68, 1.46, 1.45, 1.30 (6 × m, 6 × 1H, 6 × –C*H*H–), 1.21 (s, 6H, 2 × –CH$_3$), 1.58, 1.37 (2 × s, 2 × 3H, 2 × –CH$_3$), –9.02 (s, 1H, Ru—H).

Acknowledgment. We gratefully acknowledge financial support from the Australian Research Council, also the Australian Government for an Australian Postgraduate Research Award (N.B.), and the University of Sydney for the award of a H. B. and F. M. Gritton Research Fellowship (B.A.M.). We wish to thank Bruker (Australia) for use of the computer program SMART.

OM920729J